Mark Smalley
Aronne Merrelli
3/9/09

General Circulation
Rotating Tank Experiments

Introduction

The two large scale flow regimes in the general atmospheric circulation, the Hadley cell and the midlatitude eddy driven circulation, can be simulated in a rotating tank by creating a radial temperature gradient. A cold source (ice water) can be placed at the center of rotation, producing a temperature distribution in the rotating tank that is equivalent to the negative meridional temperature gradient on Earth. The transition between the symmetric (Hadley) regime and the eddy dominated regime can be effected by changing the rotation speed. Slow rotation speeds favor the Hadley regime, and fast rotation speeds favor the eddy regime. The transition is qualitatively similar to the actual transition in the subtropics, where the zonal flow speed in the tropical jet because large enough to create instabilities that are partly responsible for midlatitude eddies.

For the Hadley regime, the radial temperature gradient is equivalent to a meridional temperature gradient in the atmosphere. The thermal wind relationship (equation 1, below) can be used to connect the temperature gradient with the vertical shear in the flow azimuthally around the tank, which is equivalent to the zonal flow of the jet stream. The flow at the bottom of the tank will be small, because of frictional stress on the fluid with the tank surface. To a first approximation, the flow at the bottom can be assumed to have zero velocity, so the vertical shear increases the zonal speed from zero to the maximum at the fluid's surface.

$$(1)\quad \frac{\partial u}{\partial z} = -\frac{g\alpha}{2\Omega}\frac{\partial T}{\partial r}$$

In the eddy dominated regime, the flow is unstable and breaks into eddies with a spatial scale related to the Rossby radius of deformation. In this regime, transport is produced by covariance between the deviations from the mean flow, u' and v', with fluctuations of fluid parameters. For example, a heat flux per specific volume, toward the center of the tank is produced by a mean covariance between the meridional speed deviation and the temperature: $\overline{v'T'}$. The covariance can be very difficult to measure, since it requires detailed, high frequency, in phase sampling of the two quantities. However, it can be estimated from the products of the two variances,

$$(2)\quad \overline{v'T'} = \rho\sqrt{\sigma_v^2\sigma_T^2}$$

if the correlation coefficient (ρ) is known. Variance measurements do not require the sampling phase to be tightly controlled, so the experimental procedure can be easier. In the case of eddy circulations within the rotating tank, this means we can simply multiply

estimates of the meridional speed and temperature variances. We do not have a direct estimate of the correlation coefficient, so this will represent an upper limit. Since eddies are ultimately driven by temperature variations, we would expect the fluctuations in temperature and speed to be correlated fairly strongly, so the correlation coefficient should be significantly larger than zero.

Given the estimate of the eddy temperature – meridional flow covariance (Eq. 2), the total heat flux can be estimated:

$$(3)\quad \frac{dQ}{dt} = \rho c_p \int \left[\oint \overline{v'T'} ds \right] dz \approx \rho c_p \sigma_v \sigma_T (2\pi r) H$$

The approximate expression assumes the covariance term is constant through the tank, so the integral reduces to the area of the cylindrical cross section in the middle of the tank – the circumference of a zonal axis through the tank ($2\pi r$) times the depth (H).

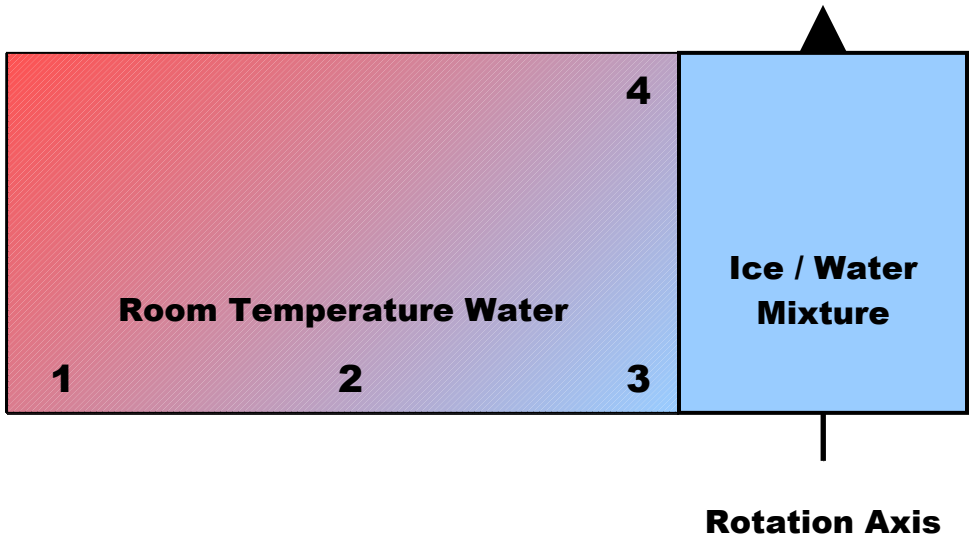

Figure 1. Cross section of the rotating tank, showing the location of the four temperature sensors, and a schematic diagram of the temperature distribution.

Experiment:

The basic experimental setup was used in all cases. Before water is added to the tank, a metal bucket of about 14 cm diameter is placed in the center, with a dense weight in order to keep the empty bucket at the bottom of the tank. Four temperature sensors were attached to the tank bottom and the side of the bucket, as shown in Figure 1. Water is then added to a depth of 10 cm, and the tank is set to a certain rotation speed and allowed to relax to solid body rotation over the course of about 15 minutes. After solid body rotation is reached, ice and water is added to the bucket, after measuring the water and ice mass. The water ensures good thermal coupling between the ice and the bulk water in the tank, by eliminating air pockets between ice cubes. The tank is allowed to adjust to the new flow regime for a few minutes. Dye and tracers are then added to

monitor and measure the flow. The same procedure was followed for three separate experiments, with rotation rates set to roughly 1, 5 and 10 RPM. Finally, the ice is weighed after the experiment, so that the total heat content change can be estimated from the latent heat of fusion for ice.

Results:

The first experiment was performed with the rotation rate set very slow (slightly less than 1 RPM). The initial main water volume in the tank was warmer than room temperature. Once the ice was added, a symmetric Hadley-like circulation was observed. Figure 2 shows the temperature history for the four temperature sensors. The largest temperature gradient was observed along the edge of the bucket, in the vertical dimension. The radial temperature gradient along the bottom of the tank was approximately 2 degrees C for the duration. Permanganate crystals show a slow outward anticyclonic flow at the lowest layer in the tank. Surface tracers show a much faster cyclonic flow at the surface, as expected from the Thermal wind relationship. A single tracer was measured for about two thirds of one full circulation using the particle tracking software. The track and speed measurement are shown Figure 3. Since the motion is very smooth, and almost entirely azimuthal (e.g., zonal), the speed measurement is a direct estimate of the desired *u* speed. Inserting the measurements into the Thermal wind relation (Equation 1) gives an estimate of 0.05 K/cm for the radial temperature gradient. The rough estimate from the temperature sensors would be about 0.15 K/cm (2 degrees over the 13 cm width of the annulus in the tank), although the temperature measurements have a significant uncertainty. In any case, the results are consistent to a factor of 3.

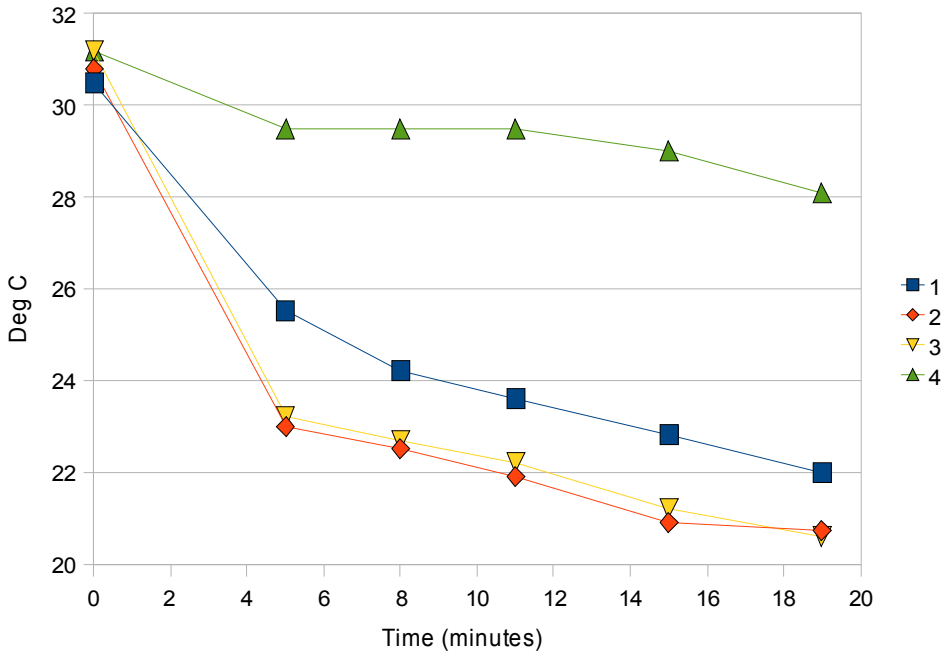

Figure 2. Time history of temperature measurements for the slow rotation (Hadley) experiment.

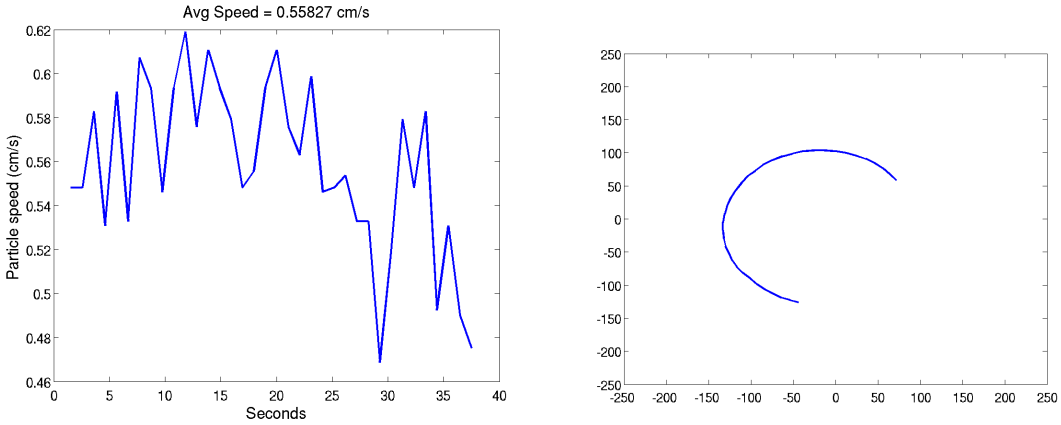

Figure 3. Particle speed (left) and path (right) for the single particle measured in the slow rotation (Hadley) experiment.

The second two experiments were run at 5 and 10 RPM. In both cases, eddies were observed, with similar spatial variation. The selected frames in Figure 4 show the eddy distributions in the two experiments, and the spatial scale is not significantly different. Figure 5 shows the temperature history for the two experiments, with the temperature sensors in the same configuration as the slow rotation experiment (Figure 1). The initial temperature of the main water mass was room temperature in these cases, so the temperature gradients are smaller. However, the general pattern is the same as the Hadley circulation case – most of the temperature change is vertical along the side of the bucket, and the radial temperature gradient along the bottom of the tank is approximately 1 – 2 degrees C.

Figure 4. Observed eddy flow patterns in the 5 RPM experiment (left) and 10 RPM experiment (right).

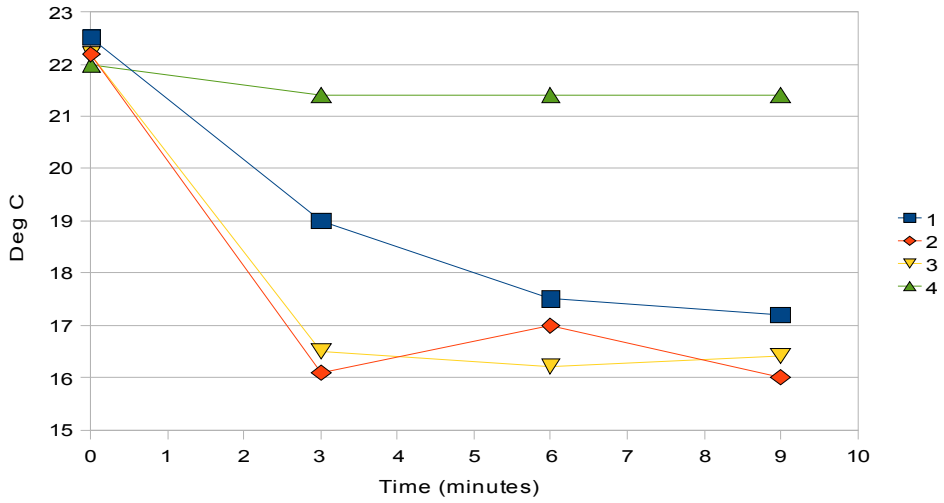

Figure 5. Temperature time history for 5 RPM experiment. The 10 RPM experiment shows a similar pattern.

Figure 6 shows tracks for several of the tracers measured in the 5 RPM experiment. The particle tracking was difficult in this case, because of the slow particle speed, and the high amount of background clutter that degraded the tracking algorithm performance. The speed measurements are magnitudes, and the rough average across the tracers is about 0.1 cm/s, as shown in Figure 6. If we assume the eddy turbulence produces velocity fields that have equal probability in all directions, the standard deviation of the fluctuation in the *v* direction will be equal to half the average amplitude (0.05 cm/s). Assuming variance for the temperature fluctuations of 1 K, the estimate for the eddy heat flux is 180 W using Eq. 3. This can be compared to 140 and 210 W for the heat flux required to melt the ice mass in the two experiments. One additional uncertainty is the heat lost by the additional water in the ice bucket. We weighed the amount water added to the bucket, and if we assume the water is room temperature at the start of the experiment, and is chilled to zero degrees C at the end, we can compute an upper bound for this heat loss. For both experiments, this heat loss was at most 50 W, which is a factor of 3 – 4 smaller than the heat content change from the ice melt.

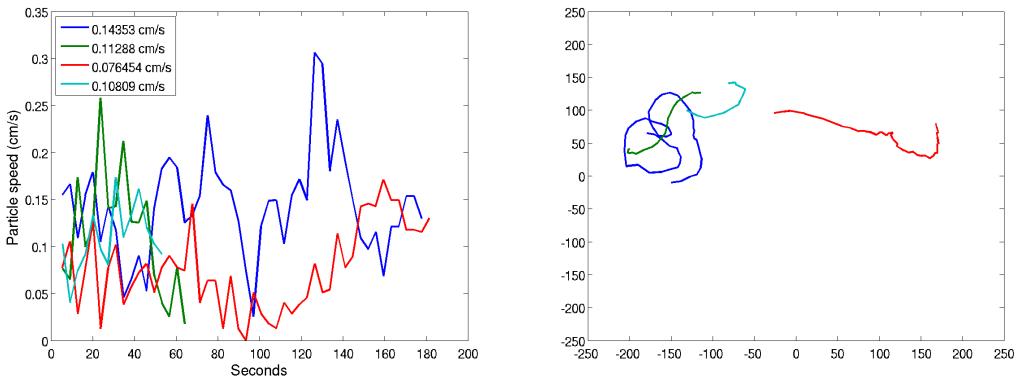

Figure 6. Measured Particle speeds (left) and tracks (right) for the 5 RPM experiment. Tracks in the 10 RPM experiment showed similar speeds.

Discussion

The slow rotation experiment successfully produced symmetric circulation analogous to the Hadley circulation. The Thermal wind relation combined with the measured velocity gradients produced an estimate of the radial temperature that was in rough agreement with the observed temperatures. Better characterization of the temperature and velocity gradients would require more measurements.

The fast rotation experiments successfully produced eddy circulations, and the inferred heat flux agreed well with the change in heat content of the ice bucket, given the experimental limitations. More precise measurements of the heat content would require better temperature measurements of the water added to the ice bucket. Better measurements of the eddy covariance would require different instrumentation to measure the time varying T', although combining it with an equally well sampled v' time series may be difficult.

Comparing our results with the flow regimes from annulus experiments in Holton 2004 (p 358, after Phillips 1963), we see rough agreement although our zones appear shifted to smaller 1/G* values (Figure 7, Table 1.). The experimental setup used to produce the chart in Holton is not exactly the same, so our setup may have different boundaries, although the general shape is similar. In each case, the thermal Rossby number was computed with a temperature delta of 1 K. The temperature range was not held at a fixed value, so it is the most poorly constrained parameter for our experimental setup.

Table 1. Non-dimensional parameters for the three rotating tank experiments.

Experiment	Rotation speed (s^{-1})	Thermal Rossby Number: $Ro_T = \frac{\alpha g H \delta T}{2\Omega^2 (b-a)^2}$	Non dimensional rotation rate: $(G^*)^{-1} = \frac{(b-a)\Omega^2}{g}$
Slow rotation (Hadley)	0.081	0.90	9×10^{-5}
Fast rotation (Eddy #1)	0.52	0.02	0.004
Fast rotation (Eddy #2)	1.1	0.005	0.015

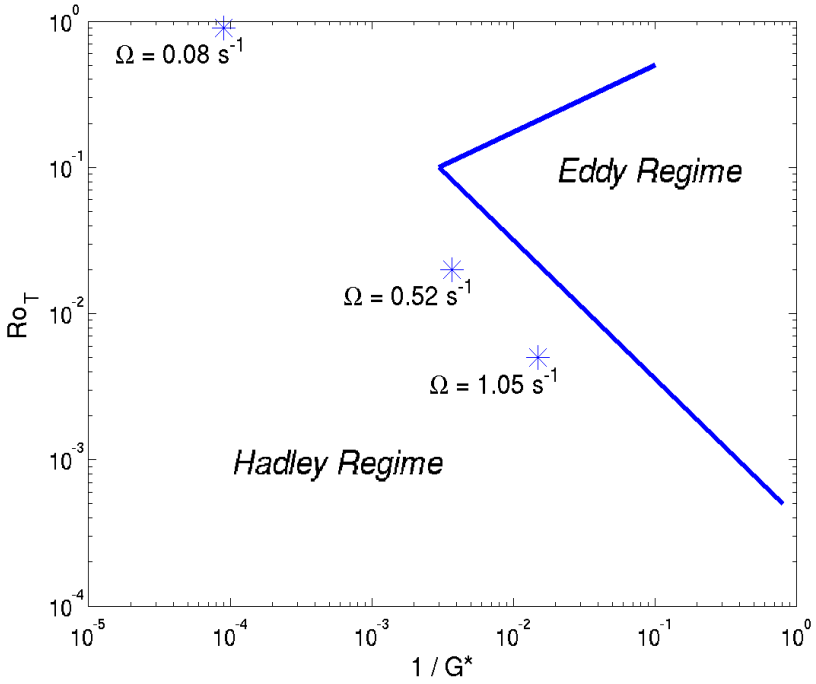

Figure 7. Flow regimes predicted by non-dimensional parameters (see Table 1). After Holton (2004).

References:

Holton, J. R. 2004: *An Introduction to Dynamic Meteorology*, 4th edition, Elsevier.
Phillips, N. A. 1963: Geostrophic motion. *Rev. Geophys.*, **1**, 123-176.